

# Synthesis and Z-scan measurements of third-order optical nonlinearity in push–pull molecules with dihydroxyethyl amino donor and nitro acceptor

Ying Qian <sup>a,\*</sup>, Guomin Xiao <sup>a</sup>, Gang Wang <sup>b</sup>, Baoping Lin <sup>a</sup>, Yiping Cui <sup>b</sup>, Yueming Sun <sup>a</sup>

<sup>a</sup> College of Chemistry and Chemical Engineering, Southeast University, Nanjing 210096, China

<sup>b</sup> Department of Electronic Engineering, Southeast University, Nanjing 210096, China

Received 7 September 2005; received in revised form 21 December 2005; accepted 4 May 2006

Available online 11 July 2006

## Abstract

Novel azo diol chromophores were synthesized through multi-step azo-coupling reaction and characterized by NMR, IR, and UV. The third-order NLO properties of the chromophores were investigated. The measurements of second hyperpolarizabilities were performed using single-beam Z-scan technique with picosecond laser pulses at 1064 nm in DMF solutions. Our results indicate that larger second hyperpolarizabilities  $\gamma$  can be readily obtained in such chromophores because of increase of molecular conjugation length and donor–acceptor conjugation path. Further enhancement of  $\gamma$  has been achieved via replacement of phenyl rings in the conjugated backbone by heteroaromatic spacers such as benzothiazole and pyrimidine rings. Therefore, it is very probable that the increase in the obtained  $\gamma$  values considerably arises from the conjugation path of the delocalized electrons for large third-order nonlinear optical effects.

© 2006 Elsevier Ltd. All rights reserved.

**Keywords:** Third-order optical nonlinearity; Z-scan; Second hyperpolarizability

## 1. Introduction

In the last decades, the nonlinear optical properties of the  $\pi$ -conjugated organic materials have been widely investigated due to their possible applications in a variety of optoelectronic and photonic applications [1–5]. While the engineering for enhancing second-order NLO efficiency is relatively well understood, the need for efficient third-order molecules and materials still exists. In third-order nonlinear optics, guidelines for the optimization of the second hyperpolarizability  $\gamma$  of a molecule have been steadily improving, but the understanding is far less developed than for first hyperpolarizability  $\beta$  [6,7]. It is desirable to optimize the  $\gamma$  values. In particular, the strong delocalization of  $\pi$ -electrons in the organic

backbone determines a very high molecular polarizability and thus remarkable third-order optical nonlinearity. In general, large hyperpolarizabilities are the result of an optimum combination of various factors such as  $\pi$ -delocalization length, donor–acceptor groups, dimensionality, conformation, and orientation for a given molecular structure [8–10].

On the other hand, Z-scan technique, introduced by Sheik-Bahae et al. [11], is an extensively utilized experimental tool for studying optical nonlinearities in a wide class of materials. The technique relies on the fact that the light intensity varies along the axis of a convex lens and is maximum at the focus. By moving the sample through the focus, the intensity-dependent absorption is measured as a change of the transmission through the sample. The nonlinear refraction is determined by the spot size variation at the plane of a finite aperture–detector combination, because the sample itself acts as a thin lens with varying focal length as it moves through the focal plane.

\* Corresponding author. Fax: +86 25 83220581.

E-mail address: [yingqian@seu.edu.cn](mailto:yingqian@seu.edu.cn) (Y. Qian).

In this paper, we designed and synthesized bifunctionalized NLO chromophores containing long conjugation aromatic chain and two hydroxyl groups, which can be directly incorporated into polymer backbones. The structures of the chromophores **1–6** are presented in Fig. 1. The third-order nonlinear optical properties of the novel azo diols have been investigated using the Z-scan technique with a 35-ps pulsed laser beam. In addition, the measurements had been made at the frequency of 1064 nm, which was of course offresonance for the molecules concerned.

## 2. Experimental

### 2.1. Materials

Di-(2-hydroxyethyl)aniline, 2-amino-6-nitrobenzothiazole, 2-aminopyrimidine, and 4-nitroaniline were obtained from Aldrich Chemical Co. *N,N*-Dimethylformamide (DMF) was dried over molecular sieves. All other solvents and chemical reagents were obtained commercially and were used as received without further purification.

### 2.2. Synthesis of azo diol

The chromophores **1–6** were synthesized by the reaction of di-(2-hydroxyethyl)aniline and the diazonium salt prepared from the respective amines.

Chromophore **1** (2-[4'-*N,N'*-di-(2-hydroxyethyl)amino-phenylazo]-6-nitro-benzothiazole) was prepared as follows. 2-Amino-6-nitrobenzothiazole (7.8 g, 40 mmol) was dissolved in concentrated sulfuric acid and glacial acetic acid at 0–5 °C. The reaction flask was immersed in an ice-bath for temperature control. Sodium nitrite (3.1 g, 45 mmol) was dissolved in cold water and added dropwise to the reaction mixture for

0.5 h under stirring. Diazonium salt was obtained and used for coupling reaction. Di-(2-hydroxyethyl)aniline (40 mmol) was added to 90 mL methanol/water (2:1) solution in a three-necked flask immersed in an ice-bath. Freshly prepared 2-amino-6-nitrobenzothiazole diazonium salt (0–5 °C) was added dropwise for 1 h to the reaction mixture under vigorous mechanical stirring. After stirring the mixture for a further 1.5 h, the mixture was neutralized with ammonia water to pH 5–6 while stirring for 0.5 h. The precipitate was filtered and dried after repeatedly washing with acetone and ethanol. The crude product was recrystallized and purified crystals were obtained. Further purification was performed by column chromatography. Yield 68%; <sup>1</sup>H NMR (DMSO):  $\delta$  = 2.52 (DMSO), 3.34 (s, 8H, CH<sub>2</sub>), 3.66 (s, 2H, hydroxyl), 7.11 (d, 1H), 7.41 (d, 1H), 7.89 (d, 1H), 8.13 (d, 1H), 8.30 (1H), 8.70 (1H), 9.05 (s, 1H). IR:  $\gamma$  (cm<sup>-1</sup>) = 3272, 1052 (hydroxy group), 2925, 2854 (–CH<sub>2</sub>–), 1712.5 (C=N), 1600 (N=N), 1508, 1336 (nitro group), 752 (C–S).

Chromophore **2** was obtained as bright purple crystals recrystallized from ethanol/water (1:1) with 70% yield. <sup>1</sup>H NMR (DMSO):  $\delta$  = 2.50 (DMSO), 3.25 (s, 8H, CH<sub>2</sub>), 3.58 (2H, hydroxyl), 6.86 (d, 2H), 7.71 (d, 4H), 7.82–7.84 (m, 4H). IR:  $\gamma$  (cm<sup>-1</sup>) = 1600 (N=N), 3399, 1029 (hydroxy group).

Chromophore **3** was synthesized in a similar way as **1**. The reaction was performed in a two-step azo-coupling process under mild circumstances. The crude product was recrystallized and purified crystals were obtained. Further purification was performed by column chromatography. Yield 50%; <sup>1</sup>H NMR (CDCl<sub>3</sub>):  $\delta$  = 1.60 (s, 8H, CH<sub>2</sub>), 3.79 (s, 2H, hydroxyl), 6.81 (2H), 7.11 (2H), 7.28 (CDCl<sub>3</sub>), 7.83 (2H), 8.33 (2H), 8.69 (2H, pyrimidine). IR:  $\gamma$  (cm<sup>-1</sup>) = 3413, 1049 (hydroxy group), 2975, 2927 (–CH<sub>2</sub>–), 1648 (C=N), 1602 (N=N), 1511, 1346 (nitro group).

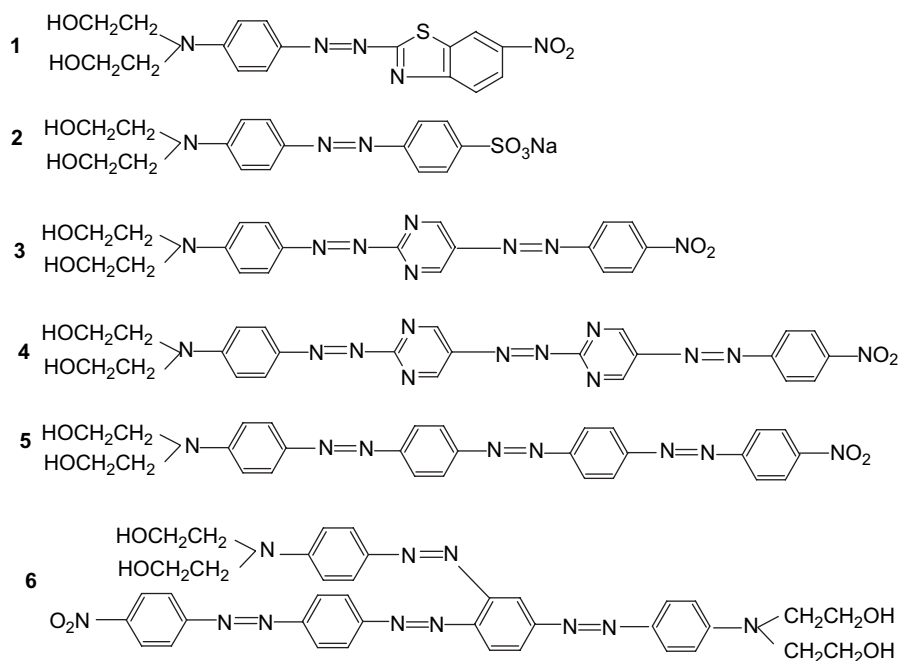


Fig. 1. Structure of azo diol chromophores **1–6**.

Chromophore **4**: Yield 44%;  $^1\text{H}$  NMR ( $\text{CDCl}_3$ ):  $\delta$  = 1.59 (s, 8H,  $\text{CH}_2$ ), 4.38 (2H, hydroxyl), 6.64 (d, 2H), 7.23 (d, 2H), 7.28 ( $\text{CDCl}_3$ ), 7.46 (d, 2H), 8.10 (d, 2H), 8.32 (2H, pyrimidine), 8.38 (2H, pyrimidine). IR:  $\gamma$  ( $\text{cm}^{-1}$ ) = 3417 (hydroxy group), 2923, 2852 ( $-\text{CH}_2-$ ), 1598 ( $\text{N}=\text{N}$ ), 1515, 1344 (nitro group).

Chromophore **5**: Yield 73%;  $^1\text{H}$  NMR ( $\text{CDCl}_3$ ):  $\delta$  = 2.19 (s, 8H,  $\text{CH}_2$ ), 4.10 (2H, hydroxyl), 6.64 (4H), 7.28 ( $\text{CDCl}_3$ ), 7.58–7.60 (4H), 8.0–8.10 (4H), 8.32–8.42 (4H). IR:  $\gamma$  ( $\text{cm}^{-1}$ ) = 3445 (hydroxy group), 1605 ( $\text{N}=\text{N}$ ), 1519, 1342 (nitro group).

Chromophore **6** was synthesized through multi-step azo-coupling reaction; each step is listed in Scheme 2. Yield 49%;  $^1\text{H}$  NMR ( $\text{CDCl}_3$ ):  $\delta$  = 2.20 (s, 8H,  $\text{CH}_2$ ), 3.64 (2H, hydroxyl), 6.82 (2H), 7.15 (2H), 7.28 ( $\text{CDCl}_3$ ), 7.60 (4H), 7.94 (2H), 8.08 (2H), 8.32 (4H), 8.41 (1H). IR:  $\gamma$  ( $\text{cm}^{-1}$ ) = 3423, 1026 (hydroxy group), 2973, 2923 ( $-\text{CH}_2-$ ), 1599 ( $\text{N}=\text{N}$ ), 1517, 1342 (nitro group).

### 2.3. Characterization

Chemical structures were identified by Fourier transform infrared spectra (FT-IR) and  $^1\text{H}$  NMR spectra. FT-IR spectra were recorded on a Nicolet 750 series in the region of 4000–400  $\text{cm}^{-1}$  using KBr pellets.  $^1\text{H}$  NMR measurements were determined with a Bruker 500 MHz apparatus, with TMS (tetramethyl silane) as internal standard and chloroform as solvent. Linear optical properties were measured by a Shimadzu UV-2201 UV-vis spectra in solution.

### 2.4. Nonlinear optical measurements

Third-order nonlinear optical properties of the sample solutions were measured by the Z-scan technique [11–13]. Measurements were performed using a Q-switched, mode-locked Nd:YAG laser source at  $\lambda$  = 1064 nm emitting  $\tau \sim 35$  ps pulses with TEM<sub>00</sub> mode at a 10 Hz repetition rate. The sample solution in a 1-mm quartz cuvette was put on a power stage and was scanned along the optical axis. The linearly polarized pulses were divided by a beam-splitter into two parts: the reflected one used as a reference to represent the incident light power and the transmitted one focused through the sample. Both the beams were recorded by two power probes simultaneously, and measured by a dual channel power meter which transferred the digitized signals to a computer. The sample was mounted on a computer-controlled translation stage that moved the sample along the  $z$ -axis with respect to the focus of the lens.

The experiments were performed at room temperature on spectroscopic-grade DMF solutions contained in a 1 mm thick quartz cell. As a reference, we performed a Z-scan on a sample of  $\text{CS}_2$ , and obtained  $n_2$ , which is in good agreement with the published results [11].

## 3. Results and discussion

### 3.1. Synthesis and characterization of azo diol

Six new azo diol chromophores were prepared by diazonium coupling reaction of the respective amines with *N*,

*N*-dihydroxyethyl aniline and further purified by column chromatography. These NLO chromophores, both with D- $\pi$ -A structure, consist of an electron-donating *N,N*-dihydroxyethyl aniline and electron-withdrawing aryl units. The synthetic procedures of chromophore **3–6** are shown in Schemes 1 and 2. The reaction was performed in a multi-step azo-coupling process under mild circumstances. We developed a useful synthetic method for long conjugated chain formation in which the core is generated from di-(2-hydroxyethyl)aniline and the diazonium salt prepared from the respective amines by a mild reaction. The method presented here is a fast, direct and elegant procedure to obtain functionalized long-chain azo chromophores. The chromophore has two active hydroxyl groups, which can be incorporated into many polymer structures.

The chemical structure of NLO chromophore containing diols was characterized with FT-IR, UV-vis and  $^1\text{H}$  NMR spectra. For all of the chromophores, the clear appearance of  $\sim 1600 \text{ cm}^{-1}$  bands, characteristic absorption of  $\text{N}=\text{N}$  stretching, indicated the existence of the azo groups. The absorption peaks at  $\sim 1515$  and  $\sim 1340 \text{ cm}^{-1}$  indicated the existence of the nitro groups. The characteristic absorption of hydroxyl groups appear at  $\sim 3400 \text{ cm}^{-1}$ .

### 3.2. Linear optical properties

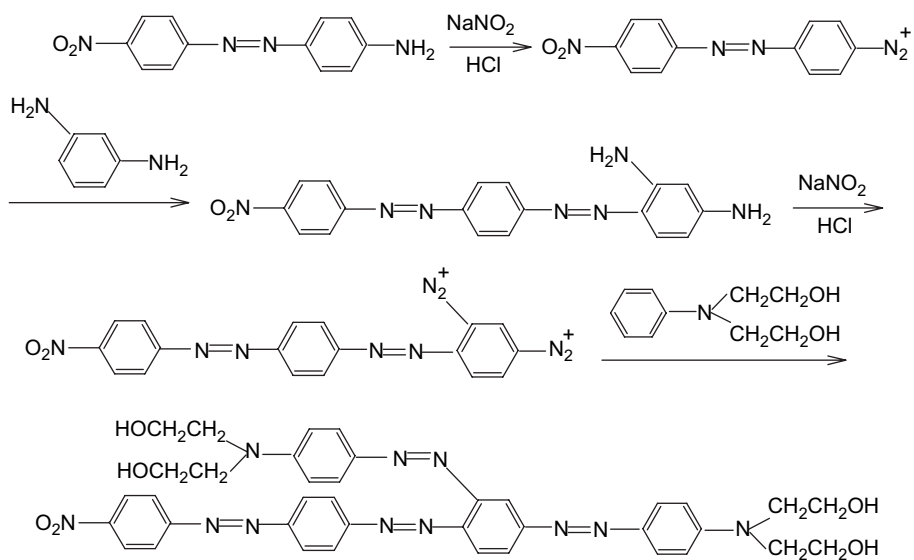
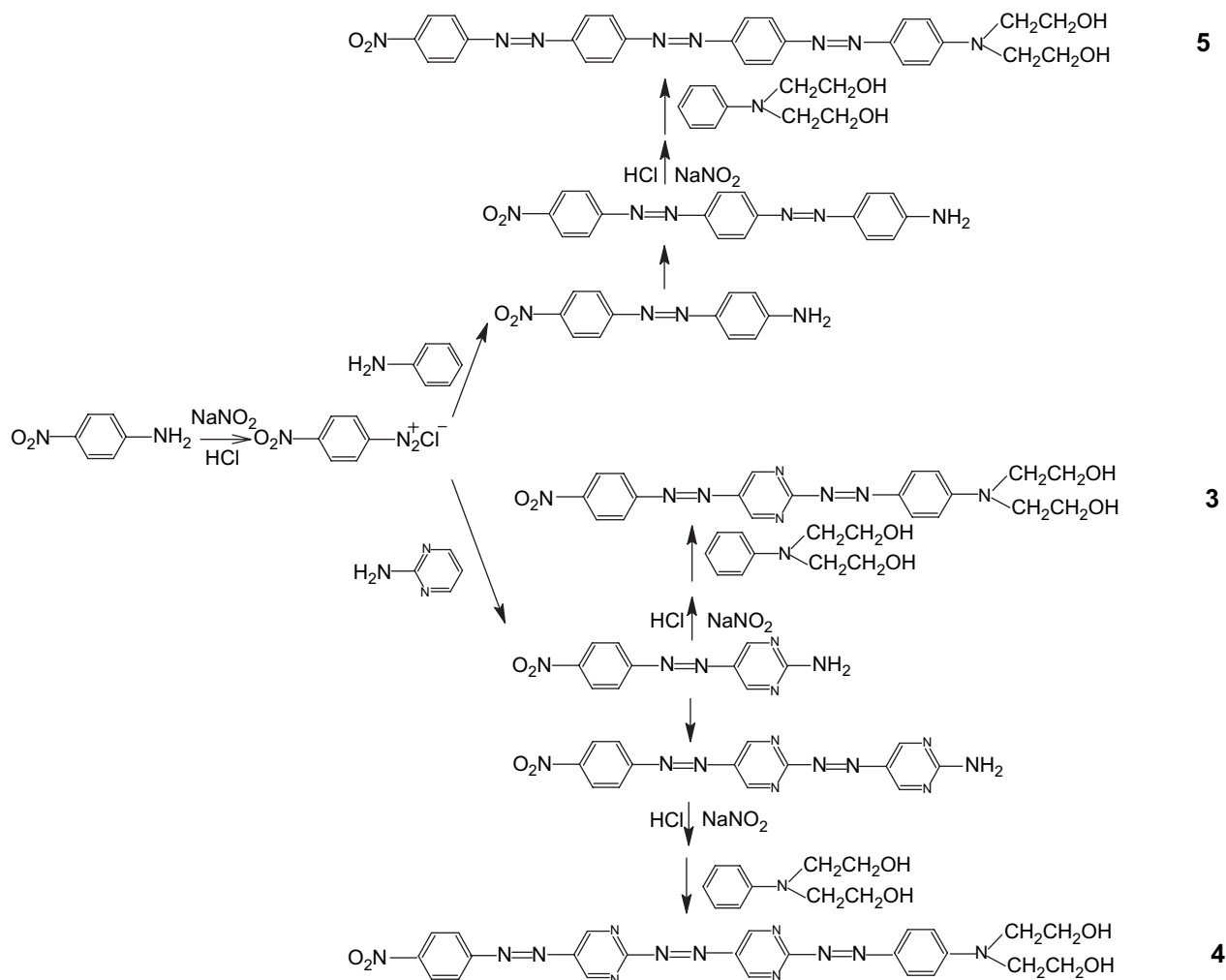
The UV-vis spectra of chromophores **1–6** are shown in Fig. 2. The UV-vis spectra of the chromophores show the absorption bands attributed to the aromatic moiety and the  $\pi-\pi^*$  transition of the azo conjugated unit. Upon comparing the absorption spectra in chromophores, it can be seen as obvious blue-shift of the absorption peak wavelength with the increase of the length of conjugation chain. This is a good property for NLO materials.

Fig. 3 shows these solvatochromic phenomena in different solvents, which is the solvent dependence of the UV-vis absorption spectrum of molecules. This result suggests that absorption changes with the polarity of different solvents.

### 3.3. Third-order optical nonlinearity of azo diol

The third-order nonlinear optical susceptibility  $\chi^{(3)}$  was determined with the Z-scan technique in a single-beam configuration [11–15]. Usually, Z-scans for a thin refractive sample with weak absorption are measured in the circumstances of a Gaussian beam propagating throughout a diaphragm behind a sample with the Gaussian profile of the resultant radial phase shift. In such conditions, two terms only of a Taylor series expansion of the resultant electric field at the diaphragm are taken. Thus, a final formula, giving a bridge between the normalized transmittance difference from peak to valley,  $\Delta T_{\text{p-v}}$ , and the on-axis refractive index change  $\Delta n_0$  in the beam waist, takes the form:

$$\Delta n_0 = \frac{\Delta T_{\text{p-v}}}{0.406(1-s)^{0.25} k L_{\text{eff}}}, \quad (1)$$



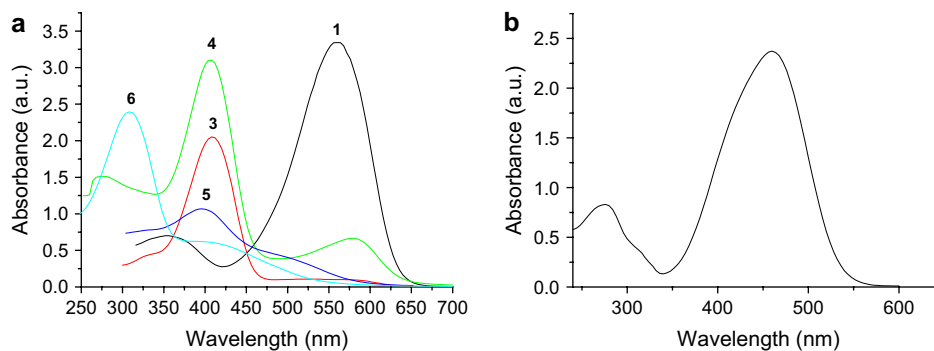


Fig. 2. UV-vis spectra of chromophores in solution (a) chromophores 1, 3, 4, 5, 6 in DMF and (b) chromophore 2 in water.

where  $s$  is the diaphragm linear transmittance,  $k = 2\pi/\lambda$ ,  $\lambda$  is the wavelength and  $L_{\text{eff}}$  is the sample effective thickness.

The real part of third-order nonlinear susceptibility  $\chi^{(3)}$  is converted from [14]

$$\text{Re}[\chi^{(3)}] = \frac{n_0^2 n_2}{12\pi^2}. \quad (2)$$

In addition, the third-order susceptibility  $\chi^{(3)}$  can be related with the second-order molecular hyperpolarizability  $\gamma$  by [13,15]

$$\text{Re}[\gamma] = \frac{\text{Re}[\chi^{(3)}]}{Nf^4}, \quad (3)$$

where  $N$  is the number of molecules per unit volume, and  $f$  is the local field correction factor according to Lorentz expression  $f = (n_0^2 + 2)/3$ .

The Z-scan measurements performed on DMF solutions of six samples reported in Fig. 4 show that nonlinear refractive index is positive giving rise to a valley-peak Z-scan curve. The curves fit to

$$\frac{T}{P_5} = 1 - 2P_3 \frac{P_1(P_4x - P_2)^2 - 2(P_4x - P_2) + 3P_1}{[(P_4x - P_2)^2 + 1][(P_4x - P_2)^2 + 9]},$$

where  $P_1 \sim P_5$  is the correlated coefficient,  $P_5$  is the normalized coefficient,  $T$  is the transmittance of Z-scan,  $x$  is the sample position along the  $z$ -axis with respect to the focus of the lens.

The second-order molecular hyperpolarizability  $\gamma$  values for six samples are also shown in Table 1.

For a more elaborate analysis of the relations between structure and second hyperpolarizabilities, one has to start

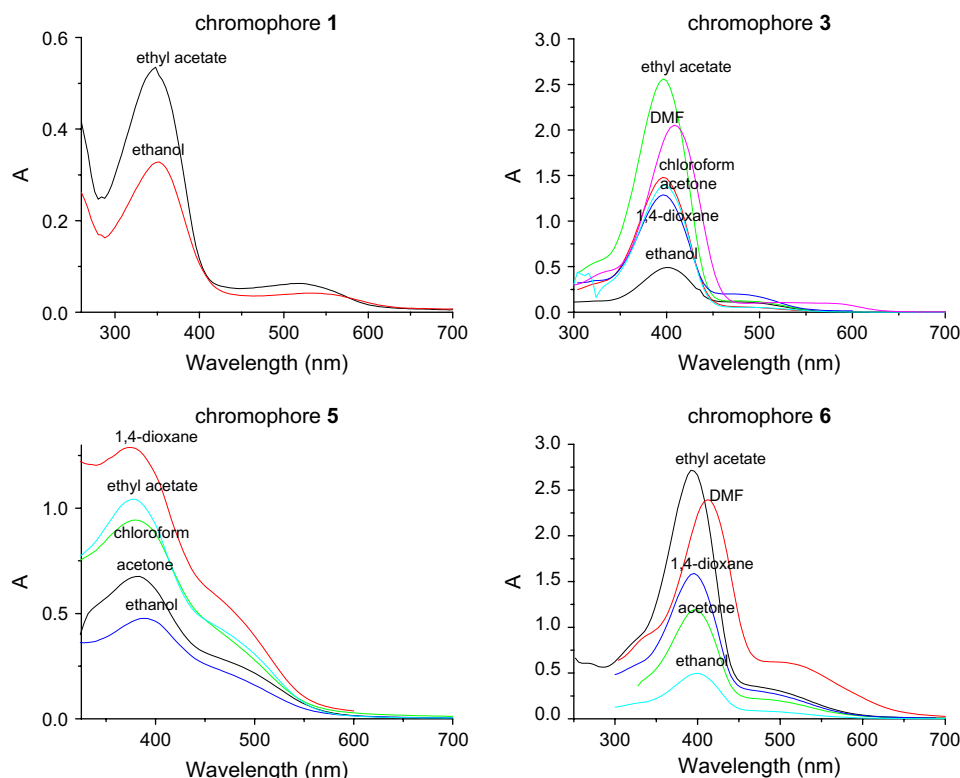


Fig. 3. UV-vis spectra of chromophores in different solvents.

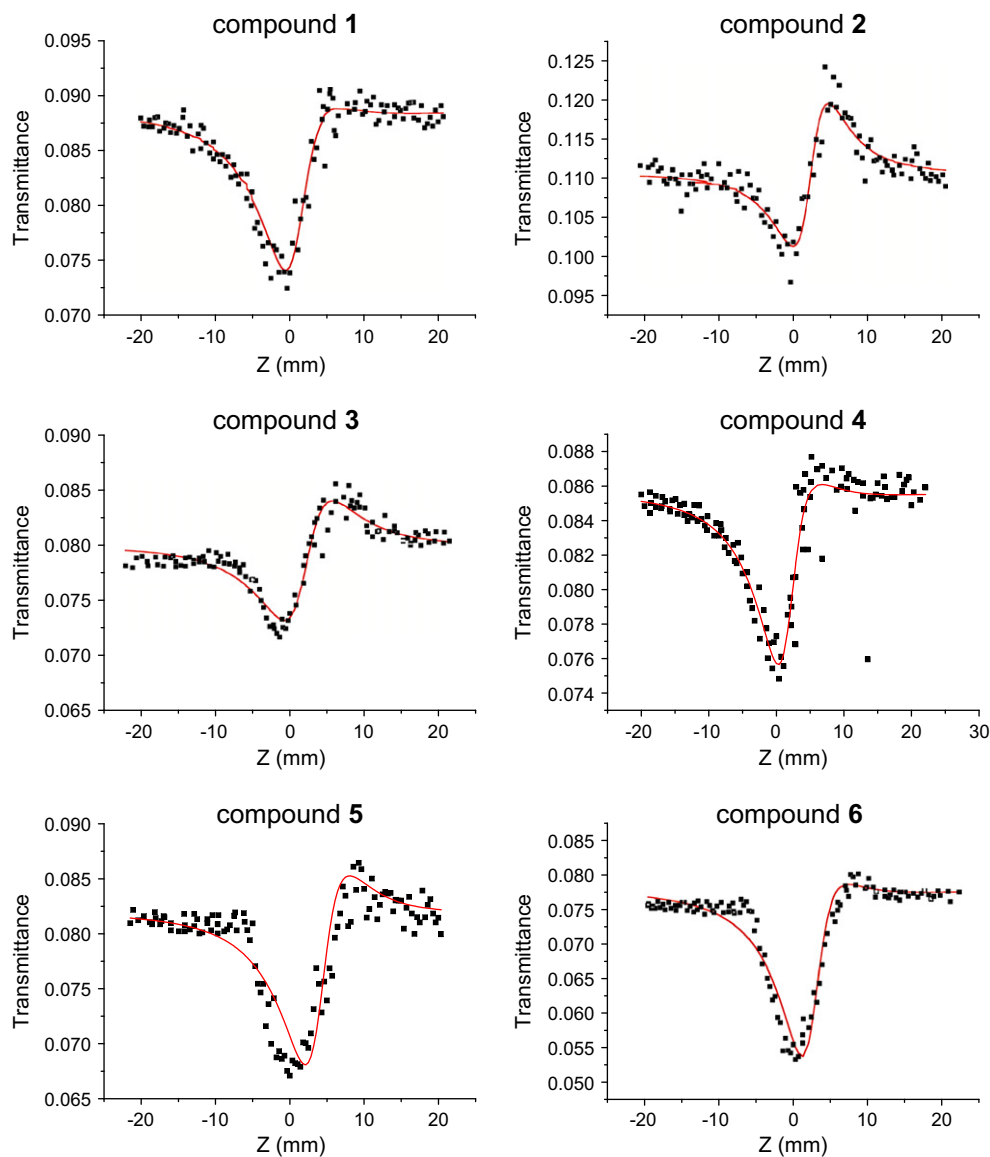


Fig. 4. Measured Z-scan of NLO chromophores 1–6.

from the electronic wave functions of a molecule. By using perturbation theory, sum-over-states expressions can be derived for the second hyperpolarizabilities  $\gamma$  by the following three-level model. For  $\gamma$ , at least three levels must be considered: the ground state and two excited states. The sum-over-states expression for the diagonal tensor element  $\gamma_{xxxx}$

and the off-diagonal element  $\gamma_{xyxy}$  of the second hyperpolarizability  $\gamma$  yields in the static limit [16–18]

$$\gamma_{xxxx} \propto -\frac{(\mu_{01}^x)^4}{E_{01}^3 N_x} + \frac{(\mu_{01}^x)^2 (\Delta\mu_1^x)^2}{E_{01}^3 D_x} + \frac{(\mu_{01}^x)^2 (\mu_{12}^x)^2}{E_{02} E_{01}^2 TP_x} \quad (4)$$

and

$$\gamma_{xyxy} \propto -\frac{(\mu_{01}^x)^2 (\mu_{01}^y)^2}{E_{01}^3 N_{xy}} + \frac{\mu_{01}^x \mu_{01}^y \Delta\mu_1^x \Delta\mu_1^y}{E_{01}^3 D_{xy}} + \frac{\mu_{01}^x \mu_{01}^y \mu_{12}^x \mu_{12}^y}{E_{02} E_{01}^2 TP_{xy}}, \quad (5)$$

where  $E_{0n}$  is the energy difference between the excited state  $n$  and the ground state 0,  $\mu_{nm}$  is the transition dipole moment between the states  $n$ ,  $m$ , and  $\Delta\mu_n = \mu_n - \mu_0$  is the difference of the dipole moments in the excited state  $n$  and the ground state.

Table 1  
Second hyperpolarizability  $\gamma$  for six samples

Sample	$\lambda_{\max}$ (nm)	$\gamma$ ( $\times 10^{-36}$ esu)
1 <sup>a</sup>	562.5	1740
2 <sup>b</sup>	459.6	1687
3 <sup>a</sup>	409.5	1305
4 <sup>a</sup>	405.6	1566
5 <sup>a</sup>	397	1827
6 <sup>a</sup>	308	2958

<sup>a</sup> Solution in DMF ( $10^{-4}$  mol/L).

<sup>b</sup> Solution in water ( $10^{-4}$  mol/L).

In Eqs. (4) and (5), sums consist of three different terms: the dipolar term  $D_i$ , the negative term  $N_i$ , and the two-photon term  $TP_i$ . However, for the present azo chromophore which has a large dipole moment at the excited state and ground state and two-photon absorption (TPA) is so little that it can be ignored, only the dipolar term  $D_i$  is expected to be dominant and can be employed for the analysis. It is clear that  $\gamma$  increases as a function of the difference in excited state and ground state dipole moments ( $\mu_1 - \mu_0$ ). A chemical transformation which increased ( $\mu_1 - \mu_0$ ) and an enhanced charge transfer faster than the other parameters in Eqs. (4) and (5) would therefore lead to an increase in  $\gamma$ .

Two-dimensional chromophore **6** with D- $\pi$ -A- $\pi$ -D structure consists of two electron-donating *N,N*-dihydroxyethyl aniline units and an electron-withdrawing nitro unit. It has two donor–acceptor conjugation paths. It is considered to have larger intramolecular charge transfer both in the ground and excited states and the increased ( $\mu_1 - \mu_0$ ). The obtained  $\gamma$  value is  $2958 \times 10^{-36}$  esu for chromophore **6**, which exhibits the largest hyperpolarizability and excellent transparency in the six chromophores.

The obtained  $\gamma$  value is  $1827 \times 10^{-36}$  esu for chromophore **5**. The  $\gamma$  value is much larger than those for chromophores **1**–**4**. The results show that  $\gamma$  increases as the length of conjugation chain increases.

From **3** to **4**, it has been shown that extended conjugation length increases the second hyperpolarizability  $\gamma$ . Benzothiazole ring is employed as the conjugating moiety between donor and acceptor substituents in chromophore **1**. Since heteroaromatic rings such as benzothiazole and pyrimidine have a lower delocalization energy than that of benzene, its substituents in donor–acceptor chromophores should be expected to result in enhanced NLO responses.

#### 4. Conclusions

We have described the synthesis and the third-order optical nonlinearities in the picosecond range of novel azo chromophores with push–pull structure. Our results indicate that larger second hyperpolarizabilities can be readily obtained in such azo chromophores because of increase of molecular conjugation length and donor–acceptor conjugation path.

Further enhancement of  $\gamma$  has been achieved via replacement of phenyl rings in the conjugated backbone by heteroaromatic spacers such as benzothiazole and pyrimidine rings. Therefore, it is very probable that the increase in the obtained  $\gamma$  values considerably arises from the conjugation path of the delocalized electrons for large third-order nonlinear optical effects.

#### Acknowledgements

This work was supported by the National Science Foundation of China No. 10374013 and the Science Foundation of Southeast University No. 9207041399.

#### References

- [1] Ma H, Jen AK-Y, Dalton LR. *Adv Mater* 2002;14:1339.
- [2] Kuhn H, Robillard J. *Nonlinear optical materials*. CRC; 1992.
- [3] Marder SR, Kippelen B, Jen AK-Y, Peyghambarian N. *Nature* 1997;388:845.
- [4] Kanis DR, Ratner MA, Marks TJ. *Chem Rev* 1994;94:195.
- [5] Zyss J. *Molecular nonlinear optics: materials, physics and devices*. Boston: Academic Press; 1994.
- [6] Bosshard Ch, Spreiter R, Gunter P, Tykwinski RR, Schreiber M, Diederich F. *Adv Mater* 1996;8:231.
- [7] Marder SR, Torruellas WE, Blanchard-Desce M, Ricci V, Stegeman GI. *Science* 1997;276:1233.
- [8] Bredas JL, Adant C, Tackx P, Persoons A. *Chem Rev* 1994;94:243.
- [9] Prasad PN, Williams DJ. *Introduction to nonlinear optical effects in molecules and polymers*. John Wiley; 1991.
- [10] Audebert P, Kamada K, Matsunaga K, Ohta K. *Chem Phys Lett* 2003;367:62.
- [11] Sheik-Bahae M, Said AA, Wei T-H, Hagan DJ, Van Stryland EW. *IEEE J Quantum Electron* 1990;26:760.
- [12] Kir'yanov AV, Barmenkov YO, Starodumov AN, Leppanen VP, Vanhanen J, Jaaskelainen T. *Opt Commun* 2000;177:417.
- [13] Zhou J, Pun EYB, Chung PS, Zhang XH. *Opt Commun* 2001;191:427.
- [14] Niu R, Zhu X, Sun Z. *Acta Optica Sinica* 2003;23:18.
- [15] Samoc M, Samoc A, Luther-Davies B, Bao Z, Yu L, Hsieh B, et al. *J Opt Soc Am* 1998;B15:817.
- [16] Gubler U, Spreiter R, Bosshard Ch, Gunter P, Tykwinski RR, Diederich F. *Appl Phys Lett* 1998;73:2396.
- [17] Audebert P, Kamada K, Matsunaga K, Ohta K. *Chem Phys Lett* 2003;367:62.
- [18] Garito AF, Heflin JR, Wong KY, Zamani-Khamiri O. *Organic materials for nonlinear optics*. London: Royal Society of Chemistry; 1989.